Proceedings of PowerGen 2012
Session 11C1, Steam Turbine Reliability, Availability and Efficiency
December 11-13, 2012, Orlando, FL

IMPROVING CORROSION FATIGUE PERFORMANCE & DAMAGE TOLERANCE OF 410 STAINLESS STEEL VIA LPB

Douglas J. Hornbach and Jeremy E. Scheel
Lambda Technologies
Cincinnati, OH USA

ABSTRACT

Corrosion fatigue (CF) and stress corrosion cracking (SCC) of stainless steel components can lead to reduced availability of steam turbines (ST). Significant operation and maintenance (O&M) costs are associated with CF and SCC prevention in both aging and new higher efficiency ST systems. Shot peening has been used to reduce the overall operating tensile stresses however corrosion pits and other damage can penetrate the relatively shallow residual compression providing initiation sites for SCC and CF. A means of reliably introducing a deep layer of compressive residual stresses in critical ST components will greatly reduce O&M costs by extending the service life of components. Low plasticity burnishing (LPB) is an advanced surface enhancement process providing a means of introducing compressive residual stresses into metallic components for enhanced fatigue, damage tolerance, and SCC performance.

High cycle fatigue tests were conducted on Type 410 stainless steel, a common alloy used in critical ST components, to compare the corrosion fatigue benefits of LPB to shot peening. Samples were tested in an active corrosion medium of 3.5% weight NaCl solution. Mechanical or accelerated corrosion damage was placed in test samples to simulate foreign object damage, pitting damage and water droplet erosion prior to testing. High cycle fatigue and residual stress results are shown. Residual compression from LPB was deeper than the damage in the samples providing a nominal 100X improvement in fatigue life compared to the shallow compression from SP. Polarization testing conducted on LPB and SP test samples are shown. The polarization results reveal a nominal 20X higher corrosion rate in the highly cold worked SP condition as compared to the lower cold worked LPB condition. Life extension from LPB offers significant O&M cost savings, improved reliability, and reduced outages for ST power generators.

KEYWORDS: Corrosion Fatigue, Residual Stress, Surface Enhancement, Low Plasticity Burnishing (LPB), Shot Peening, and 410 Stainless Steel

INTRODUCTION

Corrosion fatigue (CF), stress corrosion cracking (SCC), and fatigue initiation from erosion damage are the primary degradation mechanisms that affect low pressure (LP) steam turbine (ST) components [1-8]. These degradation mechanisms result in reduced hardware reliability, increased inspection, and significant costs to the plant.

A surface layer of beneficial residual compressive stresses in metallic components has long been recognized [9-12] to enhance fatigue strength. Shot peening is widely used in the automotive and aerospace industries, including gas and steam turbines. Other surface treatments including low plasticity burnishing (LPB) [13], laser shock peening (LSP) [14] and ultrasonic peening [15] can produce deeper compression with less cold working of the surface than shot peening. Reduced cold working improves the thermal and mechanical stability of the beneficial compression in service [16]. Studies have also demonstrated that reduced cold working reduces the likelihood and rate of corrosion [17-20].

Low plasticity burnishing (LPB) has been shown to provide a deep surface layer of high magnitude compression in aluminum, titanium, nickel alloys and steels to mitigate fatigue damage mechanisms including foreign object damage (FOD), [21-23] fretting, [24, 25] and corrosion fatigue [26-29]. The LPB process is performed on conventional CNC machine tools and robots at costs and speeds comparable to conventional machining. Application of LPB to mitigate gas turbine compressor blade FOD [30] and dovetail fretting [31] has been described in previous publications.

Corrosion fatigue and SCC research has typically focused on alloy chemistry, microstructure control, and chemical modification or coating of the surface. The current study investigates the use of compressive residual stress imparted by LPB to mechanically suppress localized stress concentrations and the cyclic SCC component of corrosion fatigue to improve the fatigue performance of Type 410 stainless steel (410 SS). 410 SS is an alloy widely used in ST applications where high strength, superior wear resistance, and corrosion resistance is required.

EXPERIMENTAL TECHNIQUE

Material and Heat Treatment

410 SS was procured in the form of a 1.0 in. (~25.4 mm) thick plate in an annealed condition per AMS 5504M. The plate was heat treated as detailed in Table I. Test samples of nominal dimensions of 0.375 x 1.25 x 8 in. (~10 x 32 x 203 mm) were machined from the plate following heat treat. Chemistry and material properties were verified after hardening and tempering. The chemistry and mechanical properties are listed in Tables II and III, respectively.

TABLE I: MATERIAL HEAT TREATMENT.

410 Stainless Steel Heat Treatment		
Process	**Temperature**	**Time**
Preheat	1450◦F (788◦C)	1 hour
Harden	1760◦F (960◦C)	1 hour
Quench in Oil	-	-
Temper	1085◦F (585◦C)	4 hours
Subcritical Quench	-120◦F (-84◦C)	-

TABLE II: MATERIAL CHEMISTRY.

410 Stainless Steel Chemistry				
Element (Weight Percent)				
C	Cr	Cu	Mn	Mo
0.13	12.16	0.16	0.59	0.10
Ni	P	S	Si	Fe
0.53	0.025	0.001	0.40	Balance

TABLE III: MATERIAL MECHANICAL PROPERTIES.

410 Stainless Steel Mechanical Properties After Heat Treatment			
Yield Strength	UTS	Elongation	Reduction of Area
113.8 ksi (785 MPa)	134.6 ksi (928 MPa)	18.5%	55.0%

Fatigue Specimen Processing

Fatigue specimens were finish machined by low stress grinding (LSG). Specimens were either LPB treated or shot peened (SP) following LSG.

LPB process parameters were developed to impart a depth and magnitude of compression sufficient to mitigate the simulated FOD with minimal cold work. Figure 1 shows fatigue specimens in the process of being LPB treated in the four-axis manipulator on the CNC milling machine.

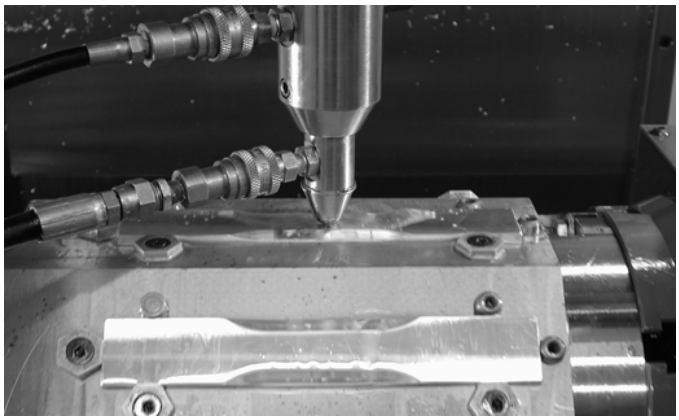

FIGURE 1: A SET OF 8 FATIGUE SPECIMENS BEING LPB PROCESSED IN A CNC MILLING MACHINE.

SP was performed using a conventional air blast peening system equipped with a rotating table with the following process parameters: 6-8A intensity, 200% coverage, and CCW14 shot. Specimens were examined optically under low magnification to confirm coverage.

To simulate surface damage from any source (handling, FOD, corrosion pitting or erosion), a surface notch with a depth of 0.01 in. (0.25 mm) was introduced by electrical discharge machining (EDM) following the LPB or SP process. Figure 2 shows an EDM notch in the gage of a fatigue sample. For a portion of the LPB treated samples a deeper notch depth of 0.02 in. (0.51 mm) was also investigated. EDM introduces a precracked recast layer in residual tension at the bottom of the notch, producing a large fatigue debit. EDM notching is widely used for reproducible laboratory simulation of high k_f damage.

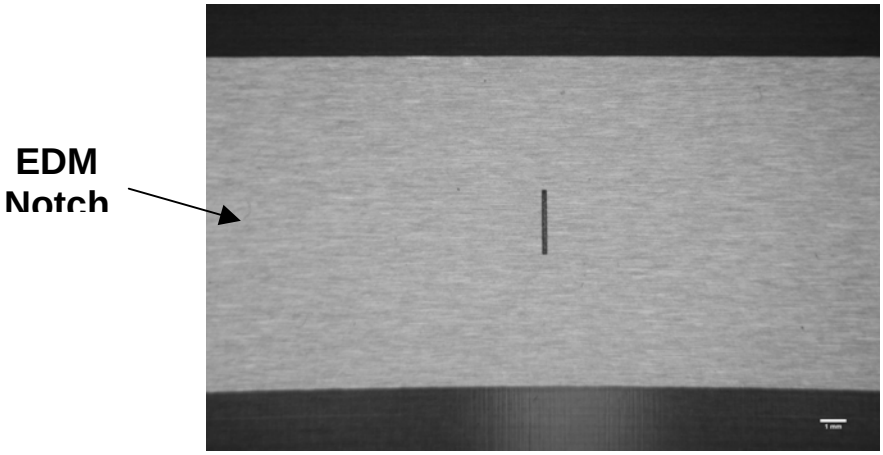

FIGURE 2: EDM NOTCH IN ACTIVE GAGE REGION OF FATIGUE SAMPLE.

High Cycle Fatigue Testing

High cycle fatigue (HCF) tests were performed under constant amplitude loading on a Sonntag SF-1U fatigue machine. A photo of the fatigue setup is shown in Figure 3.

Fatigue testing was conducted at ambient temperature (~72°F / 22°C) in four-point bending. The cyclic frequency and stress ratio, R ($\sigma_{min}/\sigma_{max}$), were 30 Hz and 0.1 respectively. Tests were conducted to specimen fracture or until "run-out" at 1 x 10^7 cycles. Specimens were subsequently broken open for optical and SEM fractographic analysis.

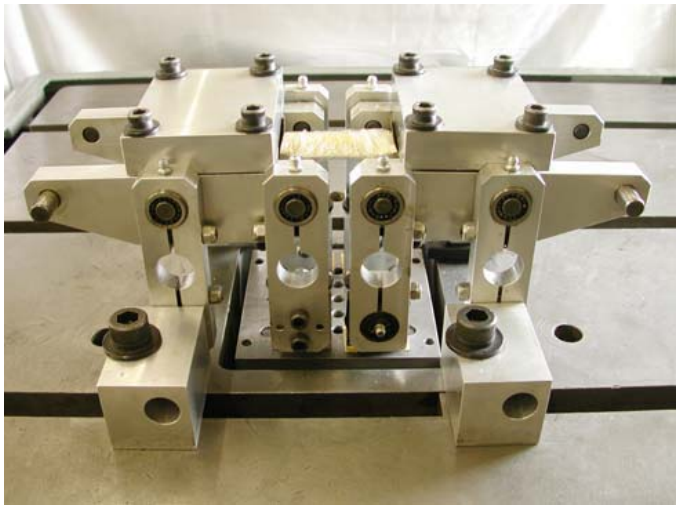

FIGURE 3: HIGH CYCLE FATIGUE TEST SET UP FOR TESTING A COMPONENT.

Fatigue samples were tested with prior exposure to SCC damage to determine the effect on the subsequent fatigue life of each material. SCC exposure tests were conducted according to ASTM Standard G39-99 and G44-99. All exposed specimens were loaded in tension to 90% of the yield strength in 4-point bending. Load was monitored continuously to detect any change in compliance. Specimens were exposed to 3.5% NaCl solution by alternate immersion (10 minutes exposed and 50 minutes unexposed per hourly cycle) for 100 hrs. Samples were then removed, cleaned with water, and tested in HCF.

Active corrosion (AC) fatigue testing was performed in a neutral 3.5% weight NaCl solution prepared with de-ionized water. Filter papers were soaked with the solution, wrapped around the gage section of the fatigue test specimens, and sealed with a plastic film to avoid evaporation.

Residual Stress Evaluation

X-ray diffraction residual stress measurements were made at the surface and below the surface to determine the depth and magnitude of residual stress distributions produced by the surface treatments. Measurements were made in the longitudinal direction of fatigue loading in the gage region employing a $\sin^2\psi$ technique and the diffraction of chromium Kα1 radiation from the (211) planes of 410 SS. The lattice spacing was first verified to be a linear function of $\sin^2\psi$ as required for the plane stress linear elastic residual stress model. [32-35]

Material was removed electrolytically for subsurface measurement in order to minimize possible alteration of the subsurface residual stress distribution as a result of material removal. The residual stress measurements were corrected for both the penetration of the radiation into the subsurface stress gradient [36] and for stress relaxation caused by layer removal [37]. The value of the x-ray elastic constants required to calculate the macroscopic residual stress from the strain normal to the (211) planes were determined in accordance with ASTM E1426-98. Systematic errors were monitored per ASTM E915-96.

Anodic Polarization Testing

Anodic potentiodynamic polarization curves were generated to characterize the effect of the SP and LPB treatments on the corrosion properties of 410 SS. A custom electrochemical cell was used to conduct the tests. The cell is based on the Avesta Cell design to prevent crevice corrosion of the specimen during testing. The open circuit potential (OCP) was recorded for each sample. Tafel slope extrapolations of the curves were used to estimate the corrosion rate for each condition. Three replicate tests were conducted for both SP and LPB conditions. All testing was performed in a neutral solution of 3.5% weight sodium chloride and distilled water according to the guidelines of ASTM G5-94. A saturated calomel electrode (SCE) was used as the reference electrode and platinum was used as the counter electrode. Testing was performed under both aerated and nitrogen purged conditions. All specimens were tested at 25° C and were pickled for 1 hour prior to measurement.

Fractography

Following fatigue testing, each specimen fracture face was examined optically at magnifications up to 60x to identify fatigue origins relative to the specimen geometry. Digital photographs were taken at 15x. A representative photograph of a typical failure for each specimen group was obtained. A few selected specimens were also examined via SEM.

Surface Roughness

The surface roughness was measured for an LPB, SP and Baseline fatigue sample. The arithmetic mean surface roughness, Ra, was determined over a 0.5 in. evaluation length parallel to the specimen axis. All reported values are the average of three measurements.

EXPERIMENTAL RESULTS

Residual Stress

The residual stress distributions are presented in Figure 4. Compressive stresses are shown as negative values, tensile as positive, in units of ksi (10^3 psi) and MPa (10^6 N/m^2). Machining produces a shallow layer of residual stress with low magnitude tension at the surface. SP produces higher surface compression of nominally -80 ksi (~ -550 MPa) at the surface. Maximum compression of -85 ksi (~ -590 MPa) occurs at a depth of approximately 0.001 in. (~0.025 mm), declining rapidly to nearly zero residual stress at a nominal depth of 0.010 in. (~0.25 mm). LPB produces surface compression of -110 ksi (~ -760 MPa), and gradually decreases to zero at a depth of approximately 0.030 in. (~0.76 mm). LPB produces a depth of compression 3X greater than SP with nominally 20% greater compressive magnitude.

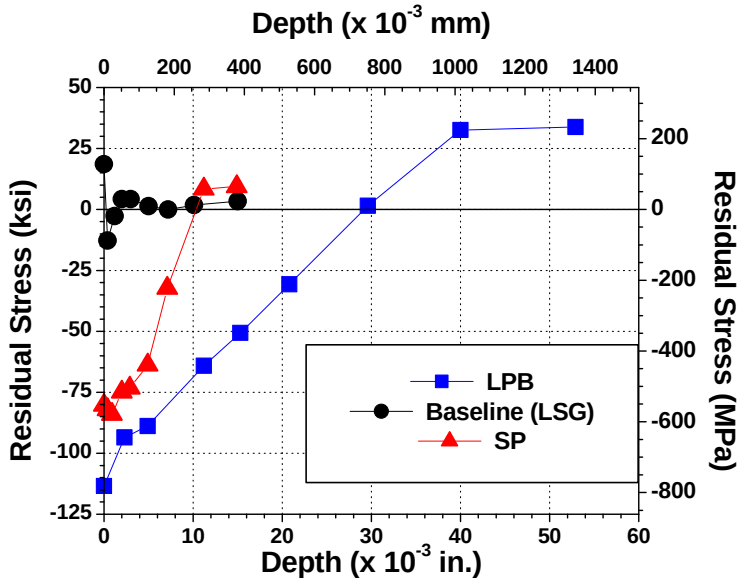

FIGURE 4: RESIDUAL STRESS PROFILES.

Damage Tolerance and Corrosion Fatigue

Figure 5 shows stress vs. life (S-N) curves for samples with an EDM notch. The baseline LSG samples with a 0.01 in. (0.25 mm) deep notch have a fatigue strength at 10^7 cycles of approximately 25 ksi (~170 MPa). Shot peened samples containing a 0.01 in. (0.25 mm) notch had a slightly higher fatigue strength, on the order of 40 ksi (~275 MPa). As is

revealed by the residual stress distributions, the 0.01 in. (0.25 mm) notch completely penetrates the compressive layer introduced by shot peening, and as a result minimizes any fatigue life benefit resulting from the shallow compression. LPB samples containing a 0.01 in. (0.25 mm) deep notch have a fatigue strength of approximately 105 ksi (~725 MPa) at 10^7 cycles, nominally 2.5X the fatigue strength of the SP samples. Tests conducted on LPB treated samples containing 0.02 in. (0.5 mm) notches reveal a fatigue strength on the order of 75 ksi (~520 MPa), nominally 2X the strength of the SP condition with a shallower 0.01 in. (0.25 mm) deep notch. LPB provides an increase in life of over 100X when compared to the SP and Baseline conditions.

Figure 6 shows the S-N curves for samples subject to prior SCC damage and fatigue tested in active corrosion. Baseline and SP samples have similar fatigue performance with maximum fatigue strengths on the order of 50 ksi (~340MPa). The results indicate a significant debit due to the pre-fatigue SCC damage and active corrosion exposure. The debit from corrosion was nearly as high as that resulting from the 0.01 in. (0.25 mm) deep notch. LPB treated samples have nominally twice the fatigue strength of the Baseline and SP samples with a fatigue strength on the order of 100 ksi (~700 MPa). LPB provides an increase in life on the order of 50X that of the SP or Baseline condition.

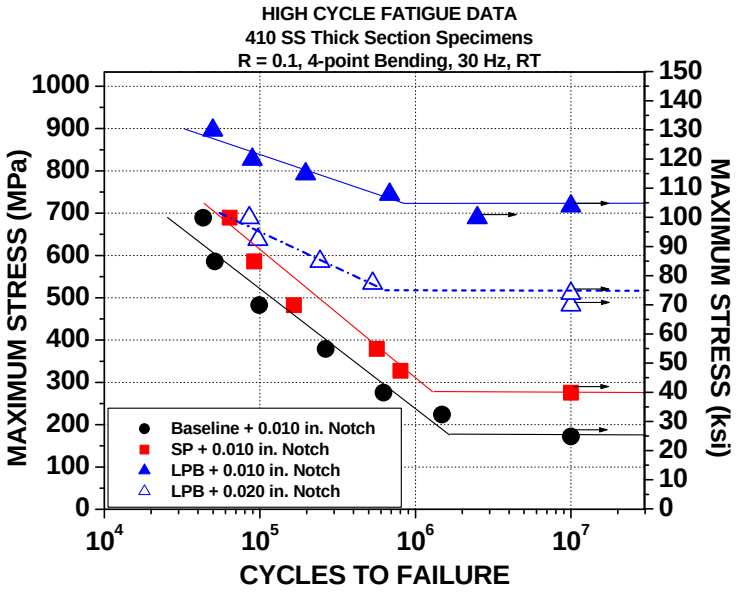

FIGURE 5: HIGH CYCLE FATIGUE RESULTS FOR SPECIMENS WITH NOTCHES.

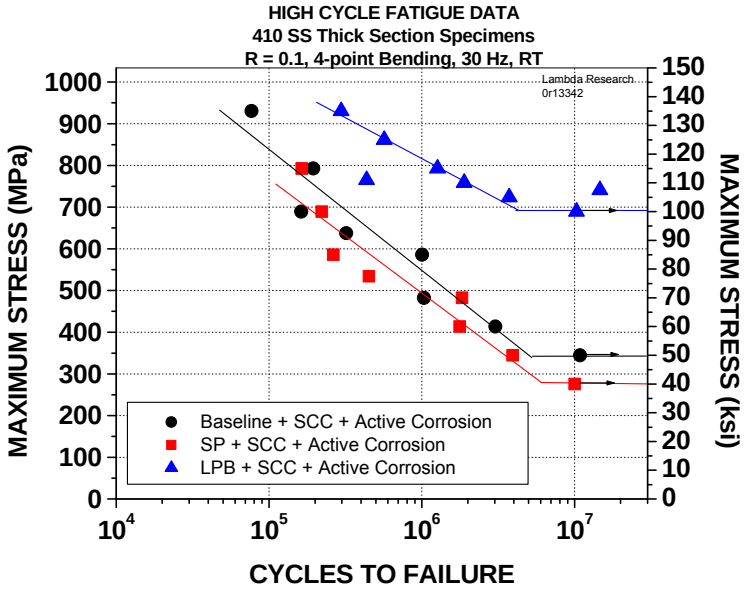

FIGURE 6: HIGH CYCLE FATIGUE RESULTS FOR SPECIMENS WITH SCC + ACTIVE CORROSION.

Anodic Polarization Testing

The results of the anodic potentiodynamic polarization tests are shown in Figure 7. Polarization curves are shown for three replicate tests on both the SP and LPB treated samples. The average open circuit potential (OCP) for the SP condition is –0.38 V, SCE and for the LPB condition it is –0.21 V, SCE. The shift in OCP indicates greater electrochemical activity and susceptibility to corrosion at the surface of the highly cold worked SP surface. Tafel slope extrapolations of the curves indicate a corrosion rate of 0.58 mils per year (14.67 microns per year) for the SP condition and 0.03 mils per year (0.79 microns per year) for the LPB condition. These data reveal the corrosion rate of the SP condition is nearly 20X higher than the LPB condition.

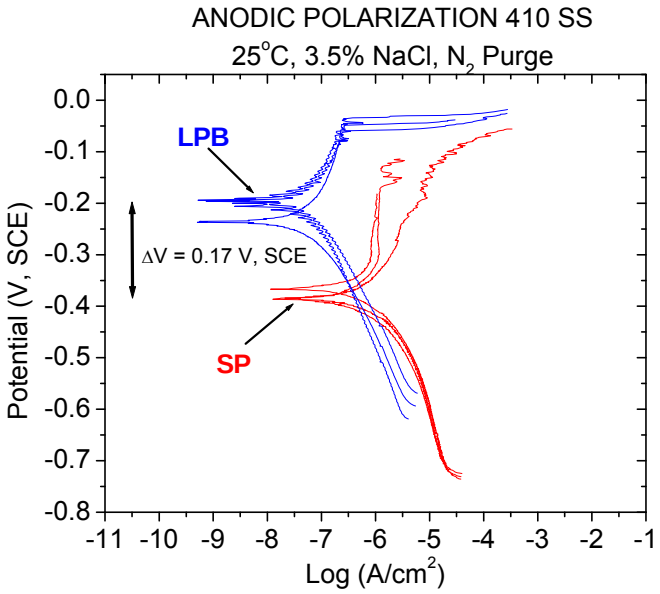

FIGURE 7: ANODIC POLARIZATION CURVES FOR SP AND LPB TREATED 410 SS. LPB TREATED MATERIAL IS MORE NOBLE AND HAS A LOWER CORROSION RATE THAN SP.

Fractography

Optical and SEM fractography indicate fatigue initiation from the bottom of the EDM notch on all of the notched samples tested. An example of a fracture face of notched samples and samples tested with prior SCC and Active Corrosion are shown in Figures 8 through 13. The location of crack initiation was similar for the various surface treatments.

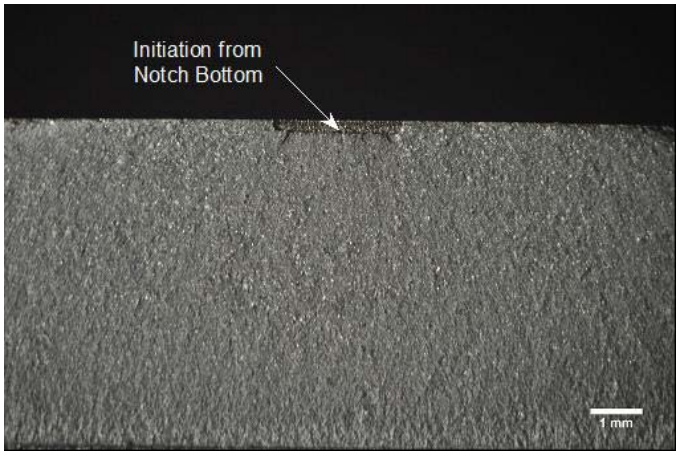

FIGURE 8: FRACTURE FACE OF BASELINE (AS-GROUND) + 0.010 IN. NOTCH SAMPLE.

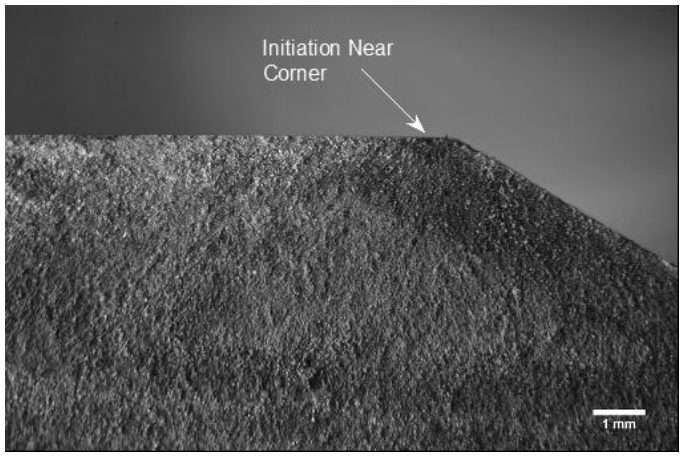

FIGURE 9: FRACTURE FACE OF BASELINE + SCC + ACTIVE CORROSION SAMPLE.

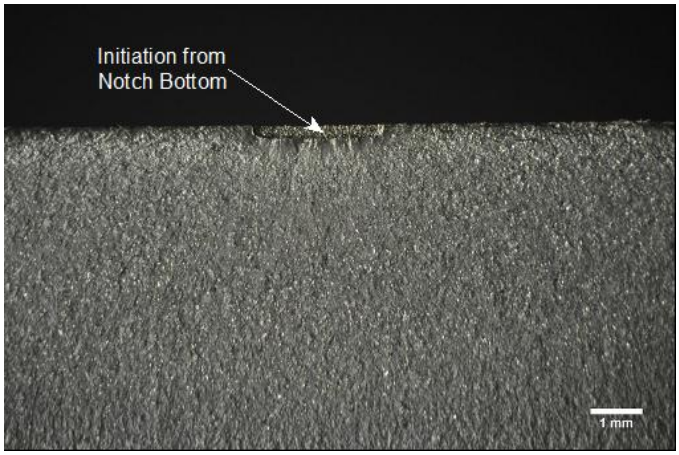

FIGURE 10: FRACTURE FACE OF SHOT PEENED + 0.010 IN. NOTCH SAMPLE.

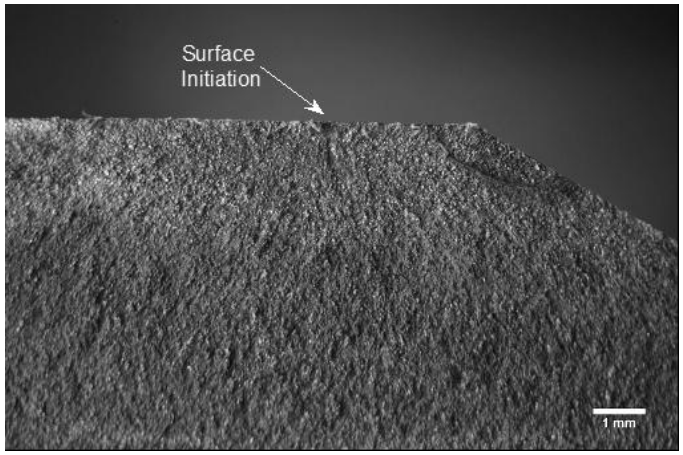

FIGURE 11: FRACTURE FACE OF SHOT PEENED + SCC + ACTIVE CORROSION SAMPLE.

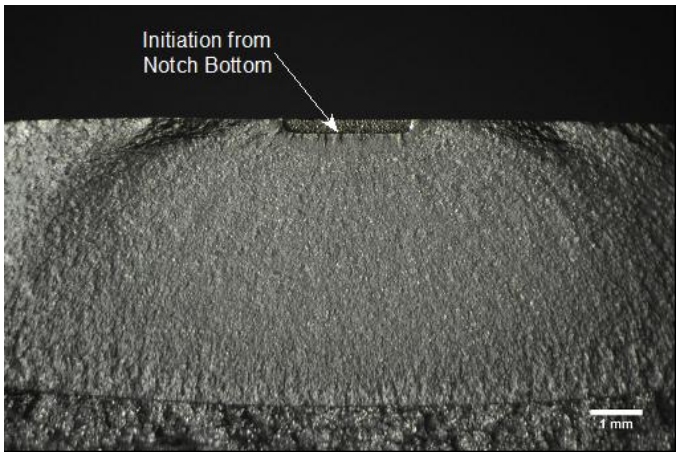

FIGURE 12: FRACTURE FACE OF LPB + 0.010 IN. NOTCH SAMPLE.

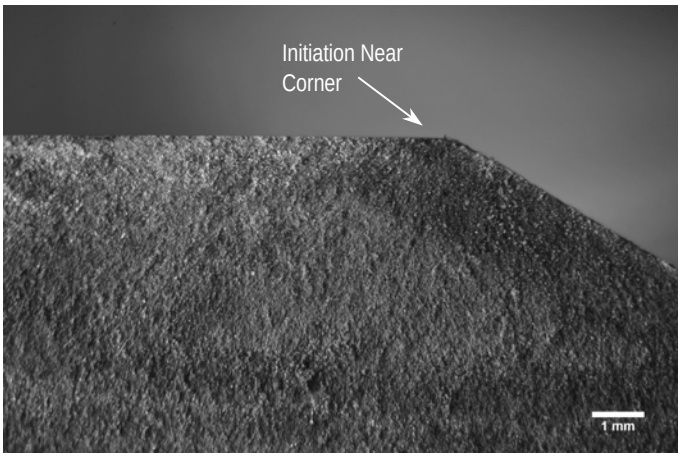

FIGURE 13: FRACTURE FACE OF LPB + SCC + ACTIVE CORROSION SAMPLE.

Surface Roughness

Results of the surface roughness measurements indicate roughness values of 19.5, 157.1, and 4.5 µin for the Baseline LSG, SP and LPB conditions, respectively. The roughness value for the SP condition is nominally 35X higher than that of LPB. Shot peening dimples produce a rough surface that can adversly impact fluid flow at the blade surface, and may require remachining or polishing to restore the surface. LPB produces a smooth work piece while avoiding the highly cold worked roughened surface of shot peening.

CONCLUSIONS

The depth of compression achievable with LPB in 410 SS exceeds that of conventional SP. For both Baseline LSG and SP specimens, the depth of compression is less than 0.010 in. (~0.25 mm), and damage with depth on that same order produces a fatigue strength of about 1/3 that of LPB treatment. The 0.030 in. (~0.8 mm) depth of LPB compression

retards initiation and growth from both 0.01 and 0.02 in. deep damage. LPB mitigates the stress corrosion effects during cyclic loading, effectively producing a fatigue strength of twice that of SP or Baseline conditions.

Anodic potentiodynamic polarization results reveal a significant shift in the OCP between LPB and SP treatments. A shift of nominally 0.17 V, SCE was observed and is a result of the difference in surface cold working between the two treatments. The highly cold worked SP condition is in a more active state leading to a corrosion rate 20X higher than that of the low cold worked LPB condition. This dramatic reduction in corrosion rate for the LPB treatment can lead to significant savings in cost and time associated with repair and replacement of ST components.

Surface roughness results show a much smoother surface for LPB treatement over SP with a 35X difference in roughness values. Shot peening dimples produce a rough surface that can adversly impact fluid flow at the blade surface.

ACKNOWLEDGEMENTS

The authors wish to thank Mr. Thomas P. Lachtrupp for his help in overseeing the residual stress measurements and Mr. Perry W. Mason for his help in conducting fatigue tests.

REFERENCES

1. Poblan-Slas, C.A., Barceinas-Sanchez, J.D.O, Sanchez-Jimenez, J.C., 2011, “Failure Analysis of an AISI 410 Stainless Steel Airfoil in a Steam Turbine,” Engineering Failure Analysis, **18**, pp. 68-74.

2. Mazur, Z., Garcia-Illescas, R., Aguirre-Romano, J., Perez-Rodriquez, N, 2008, “Steam Turbine Blade Failure Analysis,” Engineering Failure Analysis, **15**, pp. 129-141.

3. Mazur, Z., Hernandez-Rossette, A., Garcia-Illescas, R., 2006, “Investigation of the Failure of the L-0 Blades,” Engineering Failure Analysis, **13**, pp. 1338-1350.

4. Das, G., Ghosh Chowdhury, S, Kumar Ray, A., Kumar Das, S, Kumar Bhattacharya, D, “Turbine Blade Failure in a Thermal Power Plant,” 2003, Engineering Failure Analysis, **10**, pp. 85-91.

5. Heyman, F. J., Swaminathan, V. P., Cunningham,, J.W., 1981, “Steam Turbine Blades: Considerations in Design and a Survey of Blade Failure,” *EPRI Report CS-1967*, EPRI, Palo Alto, CA.

6. Carter, C.S., Warwick, D.G., Ross, A.M., Uchida, J.M., 1971, Corrosion, **27**, pp. 190.

7. Thompson, R.M., Kohut, G.B., Candfield, D.R., Bass, W.R., 1991, “Sulfide Stress

Cracking Failures of 12Cr amd 17-4 PH Stainless Steel Wellhead Equipment", Corrosion, **47**, pp. 216.

8. Swaminathan,, V.P., Cunningham, J.W., 1983, *Corrosion Fatigue of Steam Turbine Blade Materials*, R.I. Jaffee eds., Pergamon Press, New York, NY, pp.3.1.

9. Frost, N.E., Marsh, K.J., Pook, L.P., 1974, *Metal Fatigue*, Oxford University Press.

10. Fuchs, H.O., and Stephens, R.I., 1980, *Metal Fatigue In Engineerin*g, John Wiley & Sons.

11. Berns, H. and Weber, L., 1984, "Influence of Residual Stresses on Crack Growth," *Impact Surface Treatment*, S.A. Meguid eds., Elsevier, pp. 33-44.

12. Ferreira, J.A.M., Boorrego, L.F.P., Costa, J.D.M., 1996, "Effects of Surface Treatments on the Fatigue of Notched Bend Specimens," 1996, Fatigue, Fract. Engng. Mater., Struct., **19** (1), pp 111-117.

13. Prevéy, P.S., Telesman, J., Gabb, T., and Kantzos, P., 2000, "FOD Resistance and Fatigue Crack Arrest in Low Plasticity Burnished IN718", Proc of the 5th National High Cycle Fatigue Conference, Chandler, AZ..

14. Clauer, A.H., 1996, "Laser Shock Peening for Fatigue Resistance, Surface Performance of Titanium", J.K. Gregory, et al, eds, The Mineral Metals and Materials Society, Warrendale, PA, pp 217-230.

15. Watanabe, T., Hattori, K., et al, 2002, "Effect of Ultrasonic Shot Peening on Fatigue Strength of High Strength Steel," Proc. ICSP8, L. Wagner eds, Garmisch-Partenkirchen, Germany, pp. 305-310.

16. Prevey, P.S., 2000, "The Effect of Cold Work on the Thermal Stability of Residual Compression in Surface Enhanced IN718", Proceedings of the 20th ASM Materials Solutions Conference & Exposition, St. Louis, MO.

17. Kelly, R.G.; Scully, J.R. et. Al, 2003, *Electrochemical Techniques in Corrosion Science and Engineering*; Marcel Dekker, Inc. New York, pp 80-106.

18. Prevey, P.S., 2011, *Metallic Article with Improved Fatigue Performance and Corrosion Resistance*. U.S. Patent # 8,033,152.

19. Songbo, Yin, D.Y., 2005, "Effects of Prior Cold Work on Corrosion and Corrosive Wear of Copper in HNO_3 and NaCl Solutions", Materials Science Engineering: A. **394**(15), pp. 266-276.

20. Foroulis, Z.A.; Uhlig, H.H., 1964, "Effect of Cold-Work on Corrosion of Iron and Steel in Hydrochloric Acid", J. Electrochem. Soc., **111** (5), pp. 522-528.

21. Prevéy, P., Jayaraman, N., Ravindranath, R., 2003, “Effect of Surface Treatments on HCF Performance and FOD Tolerance of a Ti-6Al-4V Vane,” Proceedings 8th National Turbine Engine HCF Conference, Monterey, CA.

22. Prevéy, P.S., Hornbach, D.J., Jacobs,T., and Ravindranath, R., 2002, “Improved Damage Tolerance in Titanium Alloy Fan Blades with Low Plasticity Burnishing,” Proceedings of the ASM IFHTSE Conference, Columbus, OH.
23. Prevéy,P.S., et. al., 2001, “The Effect of Low Plasticity Burnishing (LPB) on the HCF Performance and FOD Resistance of Ti-6Al-4V,” Proceedings: 6th National Turbine Engine High Cycle Fatigue (HCF) Conference, Jacksonville, FL.

24. Shepard, M., Prevéy, P., Jayaraman, N., 2003, “Effect of Surface Treatments on Fretting Fatigue Performance of Ti-6Al-4V,” Proceedings 8th National Turbine Engine HCF Conference, Monterey, CA.

25. Prevéy, P.S. and Cammett, J.T.., 2002, “Restoring Fatigue Performance of Corrosion Damaged AA7075-T6 and Fretting in 4340 Steel with Low Plasticity Burnishing,” Proceedings 6th Joint FAA/DoD/NASA Aging Aircraft Conference, San Francisco, CA,.

26. Jayaraman, N., Prevéy, P.S., Mahoney, M., 2003, “Fatigue Life Improvement of an Aluminum Alloy FSW with Low Plasticity Burnishing,” Proceedings 132nd TMS Annual Meeting, San Diego, CA.

27. Prevéy, P.S., and Cammett, J.T., 2002, “The Influence of Surface Enhancement by Low Plasticity Burnishing on the Corrosion Fatigue Performance of AA7075-T6,” Proceedings 5th International Aircraft Corrosion Workshop, Solomons, Maryland.

28. Cammett, J.T., and Prevéy, P.S., 2003, “Fatigue Strength Restoration in Corrosion Pitted 4340 Alloy Steel Via Low Plasticity Burnishing.” Retrieved from www.lambda-research.com

29. Prevéy, P.S., 2000, "Low Cost Corrosion Damage Mitigation and Improved Fatigue Performance of Low Plasticity Burnished 7075-T6", Proceedings of the 4th International Aircraft Corrosion Workshop, Solomons, MD.

30. Prevey, P., Ravendranath, R., Shepard, M., Gabb, T., 2003, “Case Studies of Fatigue Life Improvement Using Low Plasticity Burnishing in Gas Turbine Engine Applications,” Proceedings of ASME Turbo Expo, Atlanta, GA.

31. Prevey, P., Jayaraman, N., Ravendranath, R., Shepard, M., 2007, “Mitigation of Fretting Fatigue Damage in Blades and Disk Pressure Faces with Low Plasticity Burnishing”, Proceedings of ASME Turbo Expo, Montreal.

32. Hilley, M.E. ed., 2003, *Residual Stress Measurement by X-Ray Diffraction*, HSJ784,

Warrendale, PA: SAE.

33. Noyan, I.C. and Cohen, J.B., 1987 *Residual Stress Measurement by Diffraction and Interpretation*, New York, NY: Springer-Verlag.

34. Cullity, B.D., 1978 *Elements of X-ray Diffraction,* 2nd ed., Reading, MA: Addison-Wesley, pp. 447-476.

35. Prevéy, P.S., 1986, "X-Ray Diffraction Residual Stress Techniques," *Metals Handbook*, **10**, Metals Park, OH: ASM, pp 380-392.

36. Koistinen, D.P. and Marburger, R.E., 1964, *Transactions of the ASM*, **67**.

37. Moore, M.G. and Evans, W.P., 1958 "Mathematical Correction for Stress in Removed Layers in X-Ray Diffraction Residual Stress Analysis," SAE Transactions, **66**, pp. 340-345.